ORIGINAL PAPER

VM
VIA MEDICA

HIPK2 attenuates bleomycin-induced pulmonary fibrosis by suppressing the Wnt/β-catenin signaling pathway

Fangfang Wang, Yanan Zhang, Jing Ren, Wencheng Yu*

Department of Respiratory and Critical Care Medicine, the Affiliated Hospital of Qingdao University, No. 16 Jiangsu Road, Qingdao 266000, Shandong, China

Abstract

Introduction. The present study aimed to investigate the effect of homeodomain interacting protein kinase 2 (HIPK2) on pulmonary fibrosis and the probable mechanisms.

Material and methods. We constructed a mouse model of bleomycin-induced pulmonary fibrosis and up-regulated the expression of HIPK2 in the lung by *in vivo* transfection. Lung tissues were collected for the detection of mesenchymal markers (α-SMA, collagen I, collagen III) and the expression of β-catenin as assessed by RT-PCR, western blot, and immunohistochemistry. Mouse lung fibroblasts (MLFs) with upregulation or downregulation of HIPK2 were successfully constructed and XAV939 was used to downregulate β-catenin expression. Then, we evaluated the activation of MLFs and the Wnt/β-catenin pathway under various conditions.

Results. The results showed that in the bleomycin-induced mouse model group, the lung alveolar structure was severely damaged, the amount of collagen fibers was increased in alveolar speta, and the expression of HIPK2 in the fibrotic area was found to be reduced. After upregulating HIPK2 in the lungs of the mouse fibrosis model we found that pulmonary fibrosis was attenuated and the expression of β-catenin and mesenchymal markers was reduced. The upregulation of HIPK2 inhibited the proliferation and migration of MLFs induced by TGF-β1, promoted apoptosis of MLFs, and reduced the expression of mesenchymal markers and β-catenin. Meanwhile, downregulation of HIPK2 promoted the proliferation and migration of MLFs, inhibited apoptosis, and promoted mesenchymal markers and β-catenin expression. XAV939 treatment of MLFs silencing HIPK2 inhibited their proliferation and activation *via* silencing HIPK2, promoted apoptosis, and reduced interstitial markers and β-catenin expression.

Conclusions. HIPK2 can attenuate bleomycin-induced pulmonary fibrosis by inhibiting the Wnt/β-catenin pathway in mouse lung fibroblasts. *(Folia Histochemica et Cytobiologica 2022, Vol. 60, No. 3, 247–259)*

Keywords: mouse; pulmonary fibrosis; mouse lung fibroblast; HIPK2; Wnt/β-catenin, XAV939

Introduction

Idiopathic pulmonary fibrosis (IPF) is a chronic, progressive fibrosis disease with unknown etiology. The incidence rises year after year [1]. It is more common in males and smokers [2]. The median survival is between 3–5 years after diagnosis. Fibroblast activation, apoptosis-proliferation imbalance, and extracellular matrix (ECM) accumulation play a key role in the pathophysiology of pulmonary fibrosis [3]. IPF still has no effective treatment. Lung transplantation is the only approach to improve patient survival [4]. The anti-fibrotic drugs nintedanib [5] and pirfenidone [6] are conditionally recommended. These drugs can slow the progression of pulmonary fibrosis but cannot effectively improve the prognosis [7]. As a result, continued research into IPF pathogenesis and identifying

*Correspondence address:

Wencheng Yu

Department of Respiratory and Critical Care Medicine, the Affiliated Hospital of Qingdao University, No. 16 Jiangsu Road, Qingdao 266000, Shandong, China

phone: +86 0532-82911306

fax: +86 0532-82911999

e-mail: ywcheng1167@126.com

new therapeutic targets will be critical in the future of IPF therapy.

Homeodomain interacting protein kinase 2 (HIPK2), a member of the conserved serine/threonine homeodomain interaction kinase family, is mainly located in the nucleus [8]. HIPK2 activates itself by auto-phosphorylation during its translation, and its activity is controlled through modulation of its expression by ubiquitin-dependent degradation [9] and non-degradative ubiquitination [10]. HIPK2 phosphorylate a diverse range of transcription factors and modulate many different basic cellular processes such as proliferation, differentiation, senescence, apoptosis [11, 12], autophagy [13], and DNA damage response [14], ultimately play roles in tumor suppression [10, 13], organ fibrosis [15–17], angiogenesis [18], and inflammation [19]. Fan *et al.* [20] found that HIPK2 regulates pro-apoptotic, pro-fibrotic, and pro-inflammatory pathways including Wnt/β-catenin in renal fibrosis. Kim *et al.* [21] demonstrated that HIPK2 can regulate Wnt signaling pathway *via* the direct phosphorylation and degradation of β-catenin. A preliminary study found that the HIPK2 gene was deleted in human lung fibroblasts derived from IPF action patients [11]. HIPK2's effect and mechanism of HIPK2 in pulmonary fibrosis have yet to be determined. This study investigates whether HIPK2 can attenuate pulmonary fibrosis by inhibiting the Wnt/β-catenin pathway *in vivo* and *in vitro*.

Materials and methods

Construction, identification, and amplification of overexpressing and interfering adenovirus vectors. The adenovirus vector overexpressing or silencing HIPK2 and its control were constructed successfully by Tianjin Saier Biotechnology Co., Ltd. They were Ad-control-GFP (MOCK), Ad-HIPK2-GFP (HIPK2hi), Ad-sh-control-GFP (normal control), Ad-sh-HIPK2-GFP (HIPK2low). These adenoviruses were identified under a fluorescence microscope after transfection into 293A cells. The titers of the four adenoviruses were 1.12×10^9, 1.25×10^9, 1.48×10^9, and 1.76 PFU/mL, respectively.

Construction of bleomycin-induced pulmonary fibrosis mice and collection of lung samples. All procedures were conducted following the Experimental Animal Ethics Committee of the Affiliated Hospital of Qingdao University. Male C57BL/6 mice, SPF grade, 8 weeks old, weighing between 18–20 g, were purchased from the Institute of Laboratory Animals, Chinese Academy of Medical Sciences, Beijing, China. Thirty mice were randomly divided into two groups, the Control group, and the Model group. Bleomycin (2 mg/kg) was injected into the trachea to construct a pulmonary fibrosis model (Model group), while the Control group was injected with the equivalent volume of normal saline, the experiment was performed as previously

described [22]. At 7, 14, and 28 days after modeling, five mice were sacrificed in each group, and lung samples were collected to evaluate the severity of pulmonary fibrosis and the expression of HIPK2 in fibrotic tissue. The left lung was fixed in 4% paraformaldehyde and then stained with HE (HE staining kit C0105, Biyuntian Company, China) and HIPK2 immunohistochemistry was carried out (Tianjin Saier Biotechnology Co., Ltd, China) (CST, Danvers, MA, USA). Another 45 C57BL/6 mice were randomly divided into 3 groups: (1) MOCK group, (2) MOCK+bleomycin group, and (3) overexpressing HIPK2+ bleomycin group (HIPK2 + bleomycin group). The pulmonary fibrosis model was established by intratracheal injection of bleomycin in the MOCK + bleomycin group and HIPK2hi + bleomycin group, while the equivalent volume of normal saline was injected into the trachea of the MOCK group as control. Subsequently, Ad-control-GFP or Ad-HIPK2-GFP adenovirus vectors were injected into mice *via* tail vein on the second day after modeling for *in vivo* transfection. The amount of virus given to each mouse was 5×10^9 PFU. Similarly, five mice were sacrificed at 7 days, 14 days, and 28 days after modeling. The left lung was also fixed in 4% paraformaldehyde and then used for HE staining (HE staining kit C0105, Biyuntian Company, China), Masson staining (Masson staining kit C0105, Biyuntian Company, China), and immunohistochemical staining of HIPK2 (Tianjin Saier Biotechnology Co., Ltd, China) or β-catenin (CST, USA). The right lung was stored at –80°C and then used for hydroxyproline content measurement, Western blotting, and Realtime-PCR.

Construction of mouse lung fibroblasts overexpressing or silencing HIPK2. Primary mouse lung fibroblasts (MLFs) were isolated, cultured, and identified as previously described [22]. MLFs in the logarithmic growth phase were inoculated into 6-well plates with 1.5×10^5 cells in each well and cultured in a DMEM medium (Gibco BRL, Gaithersburg, MD, USA) containing 10% fetal bovine serum (FBS). After 24 h, the fusion degree of MLFs was about 40% as assessed under an inverted microscope (Olympus Corporation, Tokyo, Japan). The cell culture medium was then removed, and MLFs were washed twice with an Opti-MEM culture medium (Invitrogen, Waltham, MA, USA). One mL Opti-MEM culture medium with 5 μg/mL Polybrene (Santa Cruz, CA, USA) was added. The multiplicity of infection (MOI) was set at 10, 20, 40, 80, and 100, and the corresponding volume of adenovirus solution was given. The cells were then cultured in an incubator containing 5% CO_2 at 37°C. After 24 h, Opti-MEM was replaced by DMEM medium containing 10% FBS. After culturing for 48 h, a fresh DMEM medium containing puromycin and 10% FBS was added. After culturing for 72 h, the infection efficiency was observed under a fluorescence microscope (Olympus, Japan). According to the different sorts of transfected adenoviruses, MLFs were divided into four groups: (1) MOCK group (MLFs transfected with Ad-control-GFP adenovirus vector), (2) HIPK2-overexpressing group (HIPK2hi group, MLFs transfected with Ad-HIPK2-GFP adenovirus vector), (3) Normal control group (NC, MLFs

transfected with Ad-sh-HIPK2-GFP), and (4) HIPK2-silencing group (HIPK2low group, MLFs transfected with Ad-sh-HIPK2-GFP adenovirus vector). To prove that HIPK2 attenuates lung fibrosis by inhibiting the Wnt/β pathway, we added Wnt/β-catenin signaling pathway inhibitor XAV939 (1 μM) to the HIPK2low group, and MLFs were grouped in another way as follows: (1) NC group, (2) HIPK2low group, and (3) HIPK-2low+XAV939 group. All MLFs were stimulated with 5 ng/mL Transforming Growth Factor-β1(TGF-β 1) (HY-P70648, Med Chem Express, USA).

Cell proliferation assay. The cell proliferation was detected by the CCK-8 detection kit (Ameresco, USA). MLFs were plated in 96-well plates at a density of 3000 cells/well and cultured for 24, 48, and 72 h respectively. 10 μL of CCK8 solution was added to each well and MLFs were then incubated for 2 h. A microplate reader (Bio-Tek, Winooski, VT, USA) was used to measure the absorbance at 450 nm (OD value). Each experiment was repeated 3 times.

Cell apoptosis assay. Annexin-V-PE/flow cytometry with an apoptosis detection kit (Shanghai Biyuntian Company, China) was used to measure the apoptotic rate of transfected MLFs. 2×10^5 cell suspension was centrifuged at 1000× g for 5 min, the supernatant was removed, and then 200 μL V-FITC binding solution was added. The cells were resuspended, 10 μL of propidium iodide (PI) staining solution was added, incubated in the dark for 10–20 min, and then tested on a FACS Calibur flow cytometer (Becton Dickinson, San Jose, CA, USA).

Cell migration assay. Lung fibroblasts migration was assessed using the Transwell method. The Transwell filter (Millipore, USA) which fits directly into the well of a 24-well plate, was seeded with 10^5 serum-starved MLFs in the upper chamber and 20% fetal bovine serum (FBS; Hyclone, Logan, UT, USA) in the lower chamber DMEM medium. The assembled assays were incubated for 48 h at 37°C with 5% CO_2. A microscope was used to quantify the number of migratory cells. Three fields were randomly selected for analysis in each experiment.

Real-time PCR. The relative mRNA expression levels of HIPK2, β-catenin, Bax, Bcl-2, capase3, collagen I, collagen III, and α-SMA in animals and cells were examined using quantitative RT-PCR as previously described [22]. Table 1 shows the primer design and synthesis. Cycle temperature parameters were 94°C for 4 min hot start and 40 cycles of 94°C for 30 sec, 56°C for 30 sec, and 72°C for 30 sec.

Western blot analysis. The relative protein expression levels of HIPK2, β-catenin, Bax, Bcl-2, caspase3, collagen I, collagen III, and α-SMA protein in animals and cells were examined by Western blot analysis, which was performed according to previously described [22]. Anti-HIPK2, anti-collagen I, anti-collagen III, and HRP-conjugated goat anti-rabbit IgG antibodies were purchased from Abcam (Santa Cruz, CA, USA). Anti-β-catenin, anti-Bax, anti-Bcl-2, anti-caspase3, anti-α-SMA, and anti-GAPDH antibodies were purchased from Tianjin Saier Biotechnology Co., Ltd., China. All pri-mary antibodies were used at a dilution of 1:1000 except for the anti-GAPDH antibody, which was diluted at 1:2000. The secondary antibody was used at a dilution of 1:20000. Primary antibody incubation was at 4°C overnight and the secondary antibody was incubated for 1.5 h at room temperature.

Immunohistochemistry (IHC). Immunohistochemical staining was used to detect HIPK2 expression in lung tissue samples as described previously [23]. Consecutive sections from each paraffin block were exposed to diluted anti-HIPK2 antibody (1:100, sc-10083, Santa Cruz Biotechnology, Inc) or anti-β-catenin antibody (1:200, ab32572, Abcam,) at 4°C overnight. Following incubation, slices were exposed to secondary antibody (1:1000, HRP-conjugated goat anti-rabbit IgG, Tianjin Saier Biotechnology Co., Ltd., China) for 1 h at room temperature. Staining was carried out by DAB kit (Zhongshan Golden Bridge Biotechnology Co. Ltd., China) according to the manufacturer's instructions. Brown particles in cells were considered positive. Immunohistochemistry of β-catenin was performed in the same way, and an anti-β-catenin antibody was purchased from CST (USA).

Hydroxyproline content determination. Hydroxyproline content was measured using a hydroxyproline assay kit (SigmaAldrich, Saint Louis, MO, USA) according to the manufacturer's instructions. A BioTek ELx800 plate reader was used to measure the absorbance ($\lambda = 560$ nm). The hydroxyproline concentration in lung homogenates was determined using a standard curve created by serial dilutions.

Statistical analysis. All the values were expressed as means ± SD. SPSS 22.0 statistical software (IBM Corp., Armonk, NY, USA) was used for analysis. Experimental data between two groups were compared with the t-test, and the three groups of data were compared one after another by the Dunnet test in one-way ANOVA. The difference was statistically significant at P < 0.05.

Results

Overexpression of HIPK2 alleviated pulmonary fibrosis

After bleomycin induction, the Model group had significantly damaged alveolar structures, thickened alveolar septa, and increased amount of collagen fibers in alveolar septa compared to the Control group (Fig. 1a). The lung injury aggravated gradually over time, reaching its peak on day 28 (Fig. 1b). On days 7, 14, and 28, immunohistochemistry of HIPK2 revealed no obvious change in the Control group, whereas the proportion of HIPK2 positive area in pulmonary fibrosis tissue was significantly reduced (Fig. 1a, c). Following bleomycin induction, severe pulmonary fibrosis emerged in the MOCK + bleomycin group, and overexpression of HIPK2 in lung tissue attenuated the severity of pulmonary fibrosis (Fig. 1d) in mice on days 7, 14, and 28. Ascroft scores increased from

Table 1. Primer sequences used for PCR analysis

Primer name	Forward primer	Reverse primer	Product length bp
HIPK2	5'CAGCAACACCAGCCCCTA3'	5'GGACTTGAAGGAGGACGAA3'	214
β-catenin	5'GGGTGCTATTCCACGACT3'	5'CCTTCTACTATCTCCTCC3'	126
Bcl-2	5'CTGAGTACCTGAACCGGCAT3'	5'GGTATGCACCCAGAGTGATG3'	174
capase3	5'GAGCTTGGAACGGTACGCTA3'	5'CCGTACCAGAGCGAGATGAC3'	234
Colla I	5'ACAGTCGCTTCACCTACAGC3'	5'GGGTGGAGGGAGTTTACACG3'	201
Colla III	5'GGCAGTGATGGGCAACCT3'	5'CCATTTCACCCTTTCCACC3'	217
α-SMA	5'GTACCCAGGCATTGCTGACA3'	5'GAGGCGCTGATCCACAAAAC3'	271
β-actin	5'CCACCATGTACCCAGGCATT 3'	5'CGGACTCATCGTACTCCTGC 3'	189

2.64 ± 0.61 to 5.42 ± 0.92 in the MOCK + bleomycin group and from 1.7 ± 0.25 to 2.9 ± 0.66 in the HIPK2 + bleomycin group (Fig. 1f). Masson staining demonstrated that blue-stained collagen was accumulated in the fibrotic tissue of the MOCK + bleomycin group, but the amount of collagen fibers decreased following HIPK2 overexpression (Fig. 1e, g). The change in hydroxyproline pulmonary content was consistent with the Ascroft score and the intensity of collagen fiber staining (Fig. 1h). The results showed that HIPK2 overexpression attenuates bleomycin-induced pulmonary fibrosis.

Overexpression of HIPK2 reduced pulmonary fibrosis by inhibiting the Wnt/β-catenin pathway

HIPK2 immunohistochemical study revealed that the proportion of HIPK2-positive area decreased in the MOCK+bleomycin group, whereas it increased significantly in HIPK2 + bleomycin group (Fig. 2a, c). Compared to the MOCK group, immunohistochemical (IHC) staining of β-catenin in the MOCK + bleomycin group was brownish yellow, while nuclear staining increased and peaked at day 28 (Fig. 2b, d). On days 7, 14, and 28, the relative expression of β-catenin, collagen I, collagen III, and α-SMA was higher at the protein and mRNA levels in MOCK + bleomycin than in the MOCK group (Fig. 2e, g–j, Table 2). Compared to the MOCK + bleomycin group, the HIPK2 + bleomycin group expressed lighter staining of β-catenin in the cytoplasm and nucleus (Fig. 2b, d). The relative expressions of β-catenin, collagen I, collagen III, and α-SMA at the protein and mRNA levels were significantly decreased and the differences were statistically significant (Fig. 2e, g–j, Table 2). Thus, overexpression of HIPK2 suppressed Wnt/β-catenin signaling pathway activation and mesenchymal markers expression in a mouse model of pulmonary fibrosis.

Construction of overexpression and interfering HIPK2 stable strains

MLFs were transfected with lentiviruses labeled with a green fluorescent protein (GFP) and HIPK2 gene fragments. MLFs were observed under a fluorescent microscope following successful transfection. Under a light microscope, we observed normal morphology of MLFs, and under a fluorescent microscope we observed green fluorescence at the optimal infection efficiency (40 MOI) (Fig. 3a). RT-PCR and Western blot analysis revealed that the relative mRNA and protein expression levels of HIPK2 were increased in the HIPK2hi group cells but decreased in the HIPK2low group cells (Fig. 3b, c). There was a statistically significant difference ($P < 0.05$).

Upregulation of HIPK2 inhibited the activation of MLFs while downregulation promoted their activation

MLFs were activated with 5 ng/mL TGF-β1, then we explored the role of HIPK2 overexpression on cell proliferation, apoptosis, and migration. In the HIPK2hi group, the number of migrated MLFs observed under a high magnification field of view was reduced (Fig. 4a, b), and the relative cell apoptosis rate was enhanced (Fig. 4c, d), and MLFs proliferation was suppressed after 24, 48, and 72 h (Fig. 4e). Simultaneously, protein and mRNA expressions of the proapoptotic factors Bax and caspase 3 were considerably enhanced, whereas signaling pathway proteins β-catenin, the anti-apoptotic factor Bcl-2, and mesenchymal cell markers collagen I, collagen III, and α-SMA were decreased (Fig. 4f–m, Table 3). In the HIPK2low group, the number of migrated MLFs increased (Fig. 4a, b), the relative apoptotic rate decreased (Fig. 4c, d), and MLFs proliferation was boosted at 24, 48, and 72 h in the HIPK2low group (Fig. 4e). Similarly, Bax and caspase 3 relative mRNA and protein expression were decreased, while β-catenin, Bcl-2, collagen I, collagen III, and α-SMA were increased (Fig. 4f–m, Table 3).
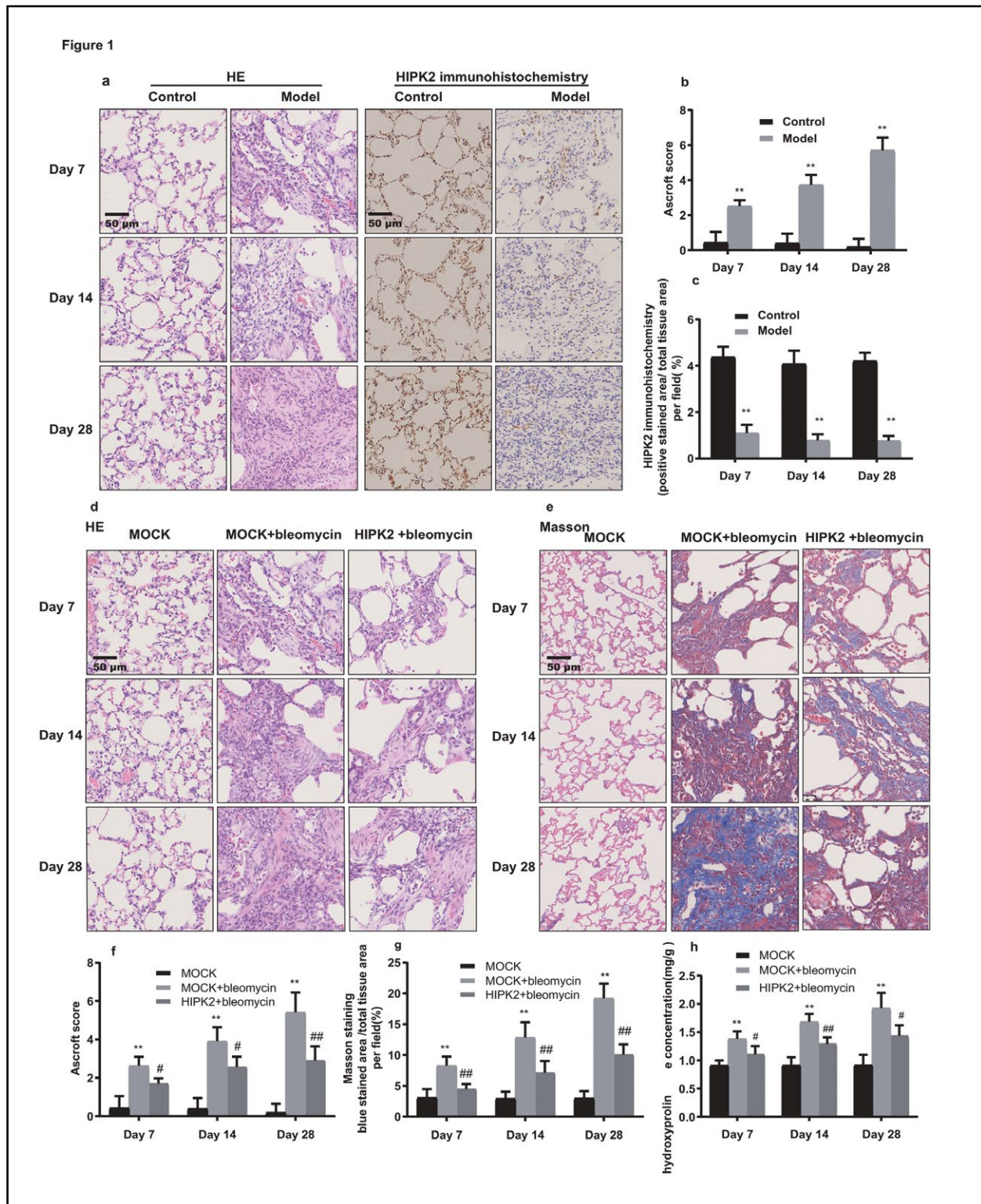
Figure 1. HIPK2 was low expressed in bleomycin-induced pulmonary fibrosis in mice, and overexpression of HIPK2 *in vivo* allevi- ated pulmonary fibrosis. HE, Masson, and immunohistochemical (IHC) stainings were performed in mice lung tissues as described in Material and methods. **A.** The alveolar structure was severely destroyed and the alveolar septa were widened after intratracheal instillation of bleomycin; HIPK2 expression in the Model group was lower than that of the Control group (scale bar: 50 μm). **B.** The Model group had a high Ascroft score. **C.** The proportion of HIPK2-positive area in pulmonary fibrosis was decreased as shown by IHC staining. **D.** HIPK2 overexpression in mice alleviated bleomycin-induced pulmonary fibrosis (scale bar: 50 μm). **E.** In the HIPK2+bleomycin group, there were fewer blue-stained collagen fibers in pulmonary fibrosis tissue than in the lungs of MOCK + bleomycin group; MOCK, MLFs transfected with Ad-control-GFP adenovirus vector (scale bar: 50 μm). **F.** Ascroft scores of the HIPK2+bleomycin group at all time points were lower than those of the MOCK + bleomycin group; **G.** The collagen-stained

area in the lungs at all time points in the HIPK2 + bleomycin group was lower than that of the MOCK + bleomycin group. **H.** Hydroxyproline concentration in lung homogenates of HIPK2 + bleomycin group at all time points was lower than that of the MOCK + bleomycin group. *, ** — compared to Control or MOCK (MLFs transfected with Ad-control-GFP adenovirus vector) group, $P < 0.05$ and $P < 0.01$, respectively; #, ## — compared to MOCK + bleomycin group, $P < 0.05$ and $P < 0.01$, respectively.

These findings indicated that HIPK2 upregulation prevented MLFs activation and accelerated apoptosis *via* Wnt/β-catenin signaling pathway, whereas downregulation of HIPK2 had the opposite effect.

HIPK2 downregulation promoted MLFs activation through the Wnt/β- catenin signaling pathway

We used the XAV939 molecule as a Wnt/β-catenin signaling pathway inhibitor [24]. MLFs were divided into three groups in the *in vitro* experiments: NC, HIPK2^{low}, and HIPK2^{low} + XAV939. We discovered that HIPK2 downregulation enhanced MLFs migration, whereas XAV939 treatment attenuated the downregulation of HIPK2 induced increase of MLFs migration (Fig. 5a). The number of migrated MLFs decreased dramatically following XAV939 intervention as seen at high magnification (Fig. 5b). Downregulation of HIPK2 protected MLFs from apoptosis, whereas XAV939 enhanced apoptosis (Fig. 5c); the HIPK2^{low} group had a lower relative apoptosis rate than the NC group, and HIPK2^{low} + XAV939 group (Fig. 5d). Downregulation of HIPK2 promoted the proliferation of MLFs, which was decreased after treatment with XAV939 (Fig. 5e). Western-blot and RT-PCR analysis revealed that the relative expression of Bax and caspase 3 were significantly lower in the HIPK2^{low} group than in the NC group, while Bcl-2, β-catenin, collagen I, collagen III, and α-SMA were significantly higher in HIPK2^{low} group than in NC group (Fig. 5f–m, Table 4).

Compared with the HIPK2^{low} group, the HIPK2^{low} + XAV939 group had higher expression levels of mRNA and protein of Bax and caspase-3 and lower Bcl-2, β-catenin, collagen I, collagen III, and α-SMA (Fig. 5f–m, Table 4). Therefore, our *in vitro* findings demonstrated that HIPK2-induced MLFs activation can be reversed by a Wnt/β-catenin signaling pathway inhibitor.

Discussion

Idiopathic pulmonary fibrosis is the most common and severe type of diffuse interstitial pneumonia [25] characterized by excessive deposition of extracellular matrix (ECM) proteins by activated lung fibroblasts and myofibroblasts, resulting in reduced gas exchange and impaired pulmonary function [26]. The pathogenesis of IPF is complex and involves the interaction of multiple signaling pathways. HIPK2 is a member of the nuclear dual-specificity serine/threonine and tyrosine kinases family, a transcriptional auxiliary regulatory protein of significant importance [12]. In recent years, as research has progressed, it has been discovered that HIPK2 plays a critical part in the pro-fibrotic and pro-apoptotic pathways. Jin *et al.* [16] demonstrated that HIPK2 mediates apoptosis and epithelial-mesenchymal transition of renal tubular epithelial cells in kidney fibrosis. He *et al.* [17] found that HIPK2 expression was significantly up-regulated in liver fibrotic tissues and TGF-β1-
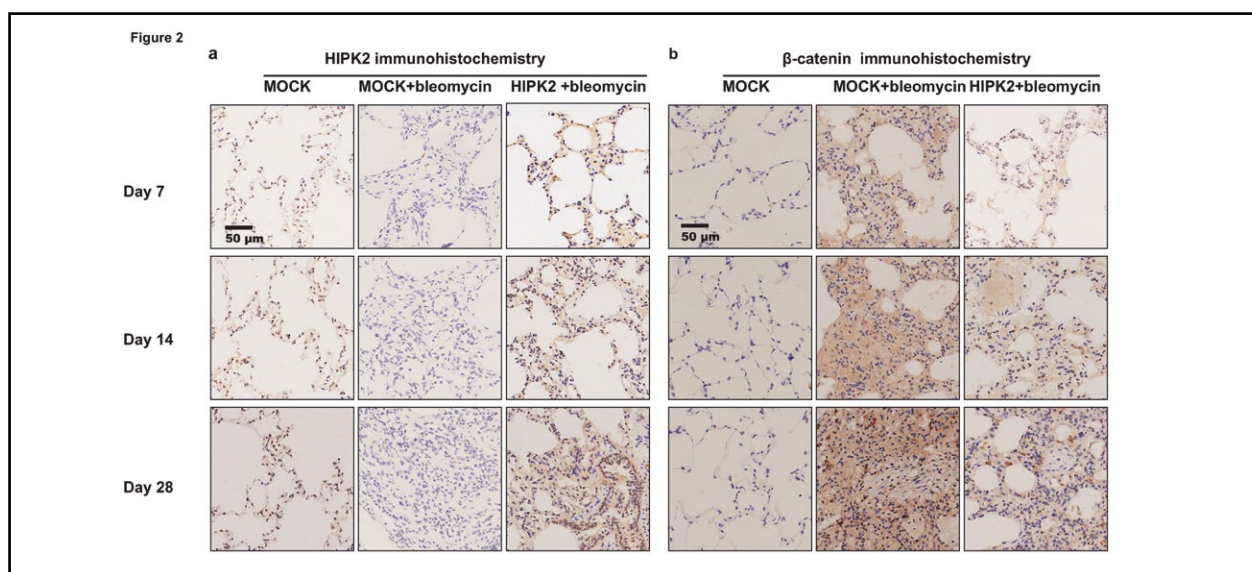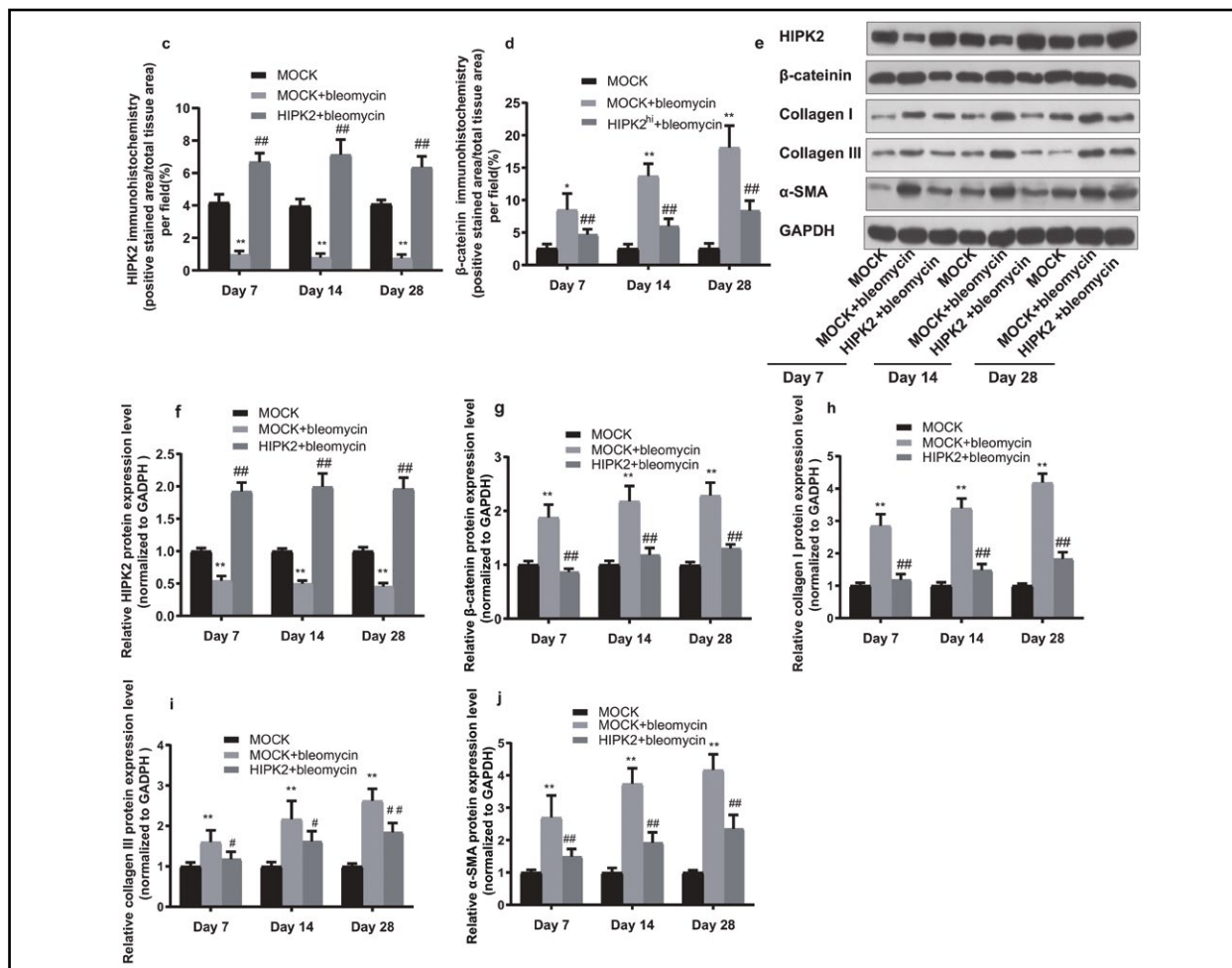

Figure 2

Figure 2. Overexpression of HIPK2 *in vivo* reduced pulmonary fibrosis by inhibiting the Wnt/β-catenin pathway. **A.** IHC staining revealed enhanced HIPK2-positive area in the HIPK2 + bleomycin group (scale bar: 50 μm). **B.** β-catenin in the MOCK + bleomycin group was brownish yellow, and positive nuclear staining increased compared to the MOCK group; however, in HIPK2 + bleomycin group, the staining became lighter and nuclear staining decreased (scale bar: 50 μm). **C.** The proportion of HIPK2-positive area was elevated in the HIPK2 + bleomycin group. **D.** The proportion of β-catenin-positive area was decreased in HIPK2 + bleomycin group in IHC staining. **E.** The protein expression levels of HIPK2, β-catenin, collagen I, collagen III, and α-smooth muscle actin (α-SMA) were assessed by Western blotting in three experimental groups at 3 time points. **F–J.** The relative protein expression levels of HIPK2, β-catenin, collagen I, collagen III, and α-SMA. *, ** — compared to MOCK group, P < 0.05 and P < 0.01, respectively; #, ## — compared to MOCK + bleomycin group, P < 0.05 and P < 0.01, respectively.

treated HSCs. However, HIPK2 function in pulmonary fibrosis remains unknown. We suspected that abnormal HIPK2 expression is associated with IPF pathogenesis. Thus, we designed *in vivo* and *in vitro* experiments to elucidate the impact of HIPK2 expression variations on bleomycin-induced pulmonary fibrosis and lung fibroblasts in mice.

We successfully developed a model of pulmonary fibrosis using bleomycin and discovered that the Model group exhibits more severe alveolar structure destruction and a lower proportion of positive area for HIPK2 IHC staining in fibrotic tissue. The result is consistent with the findings of Ricci *et al.* [11] who confirmed that lung fibroblasts from IPF patients have low HIPK2 protein and mRNA expression levels.

Therefore, we boosted HIPK2 expression in lung tissue and found that HIPK2 + bleomycin group had lower pulmonary fibrosis severity, collagen fiber staining intensity, and hydroxyproline content. These results demonstrate that lentiviral *in vivo* overexpression of HIPK2 reduces the severity of bleomycin-induced pulmonary fibrosis. Previous studies have found that HIPK2 knockdown can promote kidney [16] or liver [17] fibrosis, which is contrary to our findings. The conflicting result may be linked to tissue-specific effects [27] or multiple signal pathways related to it, and the mechanism is still unclear.

The Wnt/β-catenin signaling pathway plays an important role in the mechanisms of fibrotic diseases [28, 29]. β-catenin is the key downstream effector in
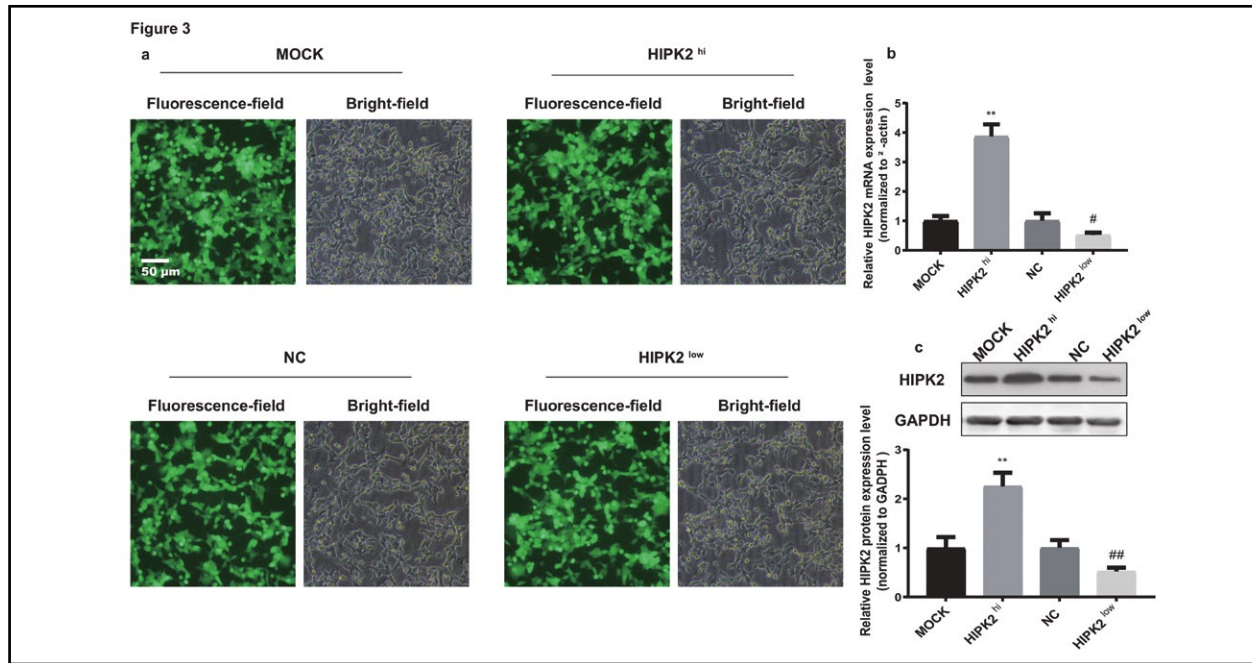
Figure 3. Construction of overexpression and knock-out HIPK2 stable mouse lung fibroblasts (MLFs) strains. **A.** MLFs showed normal morphology under the light microscope, and green fluorescence in transfected cells was detected under a fluorescent microscope at the optimal transfection efficiency [40 MOI, (scale bar: 50 μm)]. **B.** The mRNA expression levels of HIPK2 in four groups of cells. **C.** The protein expression levels of HIPK2 in the four groups. MOCK, MLFs transfected with Ad-control-GFP adenovirus vector; HIPK2^{hi}, MLFs transfected with Ad-HIPK2-GFP adenovirus vector; NC, MLFs transfected with Ad-sh-control-GFP vector; HIPK2^{low}, MLFs transfected with Ad-sh-HIPK2-GFP adenovirus vector.

Table 2. Relative mRNA expression levels of HIPK2, β-catenin, and mesenchymal markers in lung tissues of mice at the three-time points

Sacrifice time	Groups	HIPK2	β-catenin	Collagen	Collagen III	α-SMA
7 Day	MOCK	1.00 ± 0.027[a]	1.00 ± 0.025[a]	1.00 ± 0.018[a]	1.00 ± 0.034[a]	1.00 ± 0.054[a]
	MOCK+bleomycin	0.44 ± 0.017	2.20 ± 0.036	2.64 ± 0.141	1.64 ± 0.041	2.43 ± 0.168
	HIPK2+ bleomycin	2.06 ± 0.033[a]	1.09 ± 0.066[a]	1.27 ± 0.084[a]	2.27 ± 0.184[a]	1.89 ± 0.119[a]
14 Day	MOCK	1.00 ± 0.049[a]	1.00 ± 0.017[a]	1.00 ± 0.042[a]	1.00 ± 0.042[a]	1.00 ± 0.016[a]
	MOCK + bleomycin	0.32 ± 0.014	2.16 ± 0.016	3.40 ± 0.183	2.10 ± 0.083	2.87 ± 0.056
	HIPK2+ bleomycin	2.10 ± 0.142[a]	1.17 ± 0.004[a]	1.78 ± 0.134[a]	0.98 ± 0.031[a]	1.76 ± 0.085[a]
28 Day	MOCK	1.00 ± 0.053[a]	1.00 ± 0.027[a]	1.00 ± 0.044[a]	1.00 ± 0.044[a]	1.00 ± 0.032[a]
	MOCK + bleomycin	0.29 ± 0.014	2.41 ± 0.028	3.89 ± 0.172	2.49 ± 0.172	3.70 ± 0.235
	HIPK2+ bleomycin	2.17 ± 0.047[a]	1.26 ± 0.149[a]	1.97 ± 0.036[a]	1.87 ± 0.136[a]	2.04 ± 0.063[a]

Data is expressed as mean ± standard deviation (n = 5); [a]compared with MOCK + bleomycin group (P < 0.01).

Table 3. Relative mRNA expression of β-catenin, apoptotic factors, and mesenchymal markers of MLFs in each group

Groups	MOCK	HIPK2[hi]	NC	HIPK2[low]
β-catenin	1.00 ± 0.095	0.64 ± 0.196[a]	1.00 ± 0.084	2.89 ± 0.118[b]
Bax	1.00 ± 0.123	2.89 ± 0.122[a]	1.00 ± 0.156	0.37 ± 0.174[b]
Bcl-2	1.00 ± 0.097	0.48 ± 0.184[a]	1.00 ± 0.184	2.15 ± 0.121[b]
Caspase 3	1.00 ± 0.104	2.05 ± 0.090[a]	1.00 ± 0.087	0.86 ± 0.130[b]
α-SMA	1.00 ± 0.103	0.48 ± 0.894[a]	1.00 ± 0.134	1.93 ± 0.231[b]
Collagen I	1.00 ± 0.087	0.49 ± 0.081[a]	1.00 ± 0.135	1.86 ± 0.129[b]
Collagen III	1.00 ± 0.173	0.52 ± 0.097[a]	1.00 ± 0.154	2.39 ± 0.093[b]

Data is expressed as mean ± standard deviation (n = 3). [a] compared with MOCK group, P < 0.01; [b]compared with NC group, P < 0.01.
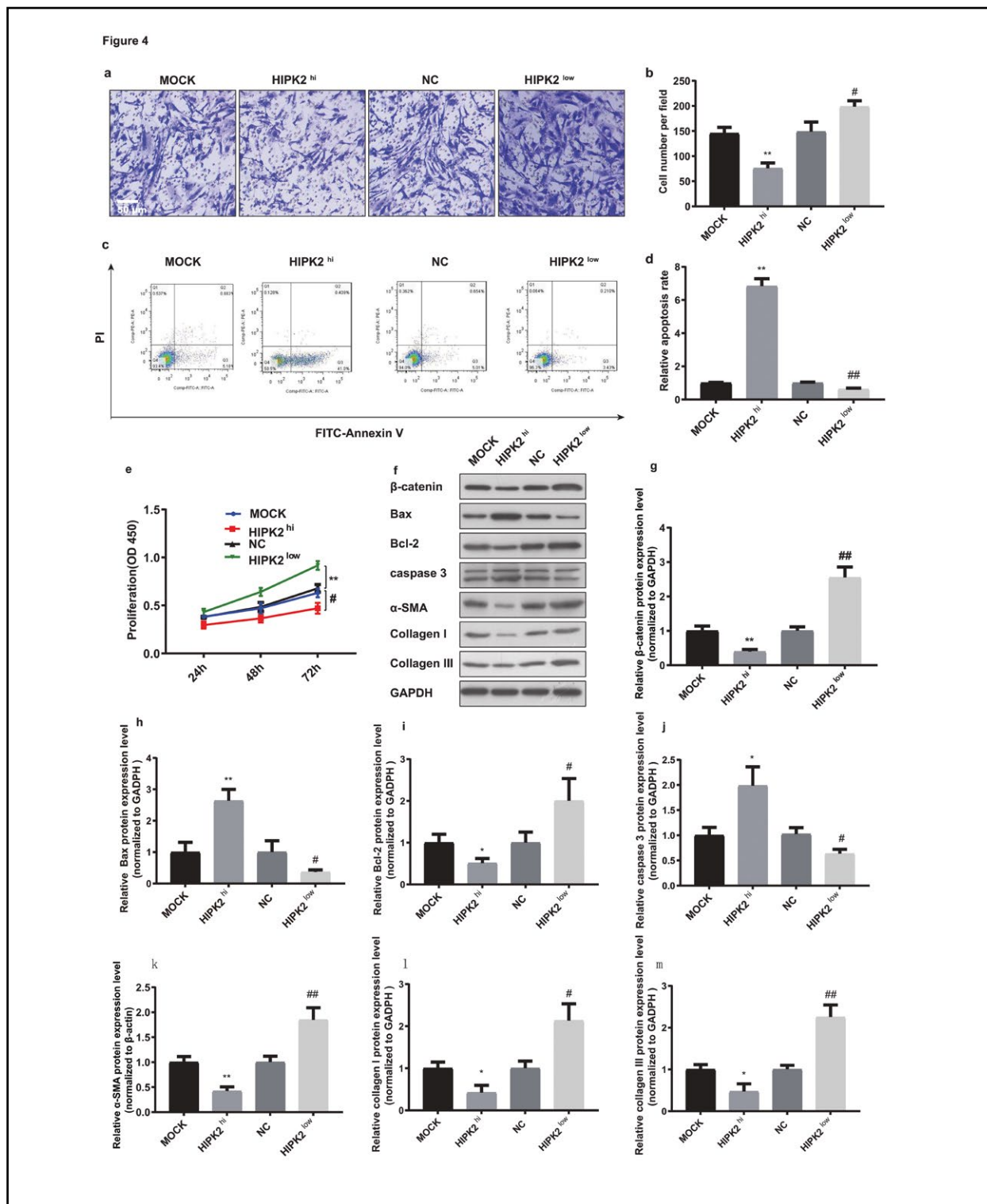
Figure 4. HIPK2 overexpression in MLFs inhibited the activation of MLFs and promoted apoptosis *via* the Wnt/β-catenin signaling pathway, while HIPK2 downregulation had the opposite effect. **A.** The view of migrated MLFs (scale bar: 50 μm). **B.** The number of migrated MLFs decreased in the HIPK2hi group while increased in the HIPK2low group compared with their controls. **C, D.** Flow cytometry revealed that HIPK2 overexpression promoted the apoptosis of MLFs; however, down-regulation led to the opposite result. **E.** HIPK2 overexpression inhibited the proliferation of MLFs at 24, 48, and 72 h, while down-regulation promoted the proliferation of MLFs. **F–M.** Western blot analysis, representative blots were shown. In the HIPK2hi group, protein expression levels of apoptotic factors Bax and caspase 3 were increased relatively, while the expression levels of β-catenin, anti-apoptotic factor Bcl-2, and mesenchymal markers collagen I, collagen III, and α-SMA were decreased; however, the levels of the studied proteins of HIPK2low group got the opposite results. *, ** — compared to the MOCK group, P < 0.05 and P < 0.01, respectively; #, ## Compared to NC group P < 0.05 and P< 0.01, respectively. Cell symbols as in the description of Fig. 3.
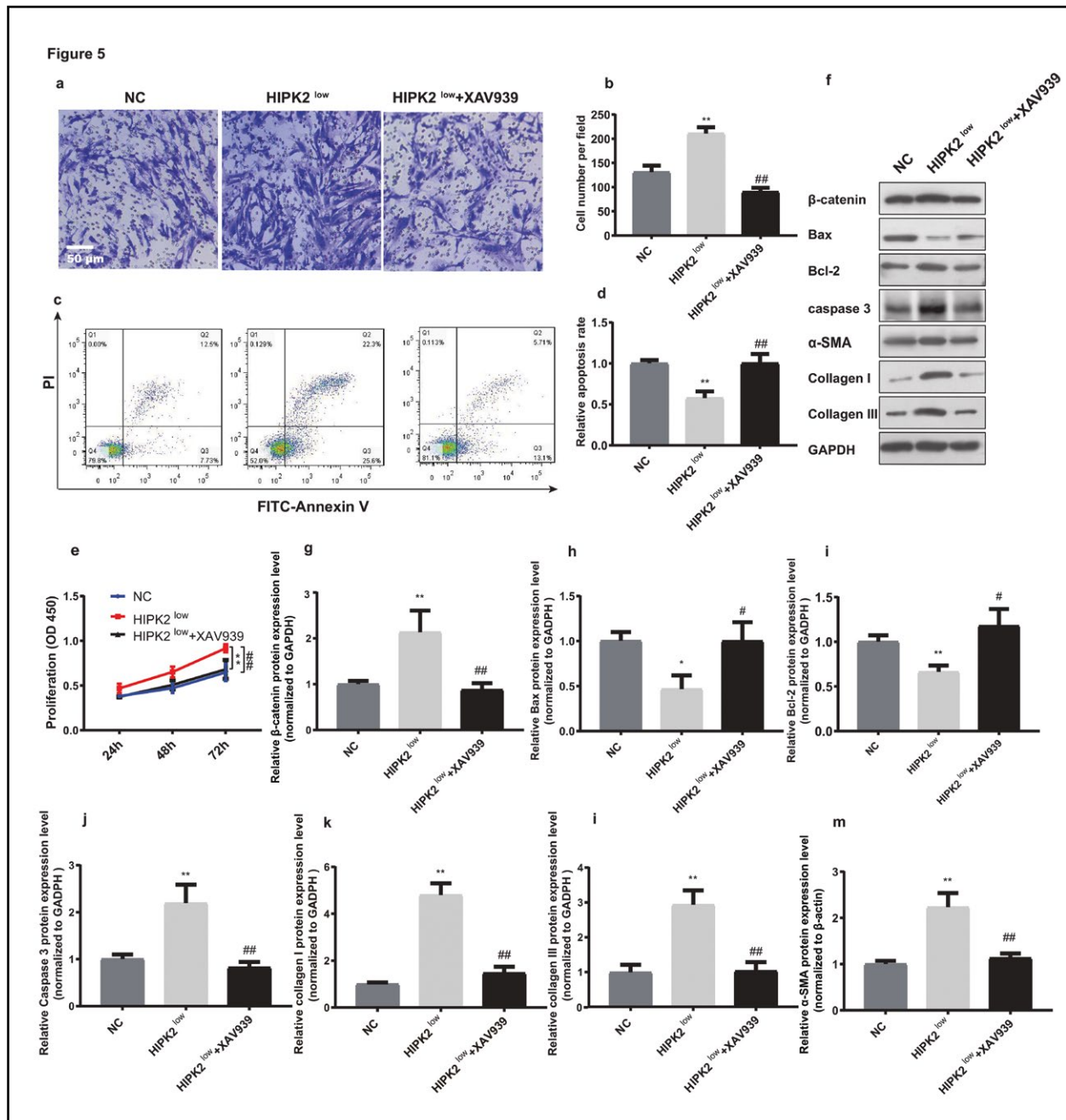
Figure 5. Wnt/β-catenin signaling pathway inhibitor XAV939 reversed MLFs activation induced by HIPK2 downregulation.
A. The view of transmembrane MLFs (scale bar: 50 μm). **B.** The number of transmembrane MLFs increased in the HIPK2^{low} group while decreased in the HIPK2^{low} + XAV939 group. **C, D.** Flow cytometry showed that the low-expression of HIPK2 protected MLFs from apoptosis, while XAV939 promoted apoptosis. **E.** HIPK2 downregulation promoted the proliferation of MLFs, and it was reversed after adding XAV939. **F–M.** Western blot analysis, representative blots were shown. Compared with the HIPK2^{low} group, the HIPK2^{low} + XAV939 group had higher expression of Bax and caspase 3 and lower expression of Bcl-2, β-catenin, collagen I, collagen III, and α-SMA. *, ** — compared to the NC group, $P < 0.05$ and $P < 0.01$, respectively; #, ## — compared to HIPK2^{low} group $P < 0.05$ and $P < 0.01$, respectively.

the Wnt/β-catenin pathway and it serves as a transcriptional co-regulator to modulate the expression of Wnt target genes [30]. Its stable accumulation in the cytoplasm and translocation into the nucleus are critical events in pulmonary fibrosis development [31].

Previous studies have established that HIPK2 triggers several pro-fibrotic, and pro-apoptotic pathways including Wnt/β-catenin in kidney fibrosis [20]. To determine the particular mechanism of HIPK2 expression alterations in pulmonary fibrosis and the

Table 4. Relative mRNA expression of β-catenin, apoptotic factors, and mesenchymal markers of MLFs after XAV939 treatment

Groups	NC	HIPK2[low]	HIPK2[low] + XAV939
β-catenin	1.00 ± 0.173[a]	2.18 ± 0.098	1.23 ± 0.127[a]
Bax	1.00 ± 0.223[a]	3.04 ± 0.149	1.28 ± 0.133[a]
Bcl-2	1.00 ± 0.202[a]	2.75 ± 0.223	1.16 ± 0.198[a]
Caspase 3	1.00 ± 0.135[a]	0.49 ± 0.224	1.21 ± 0.117[a]
α-SMA	1.00 ± 0.163[a]	2.26 ± 0.235	1.17 ± 0.090[a]
Collagen I	1.00 ± 0.090[a]	4.64 ± 0.174	1.56 ± 0.136[a]
Collagen III	1.00 ± 0.103[a]	3.04 ± 0.140	1.13 ± 0.152[a]
Data are expressed as mean ± standard deviation (n = 3). [a]Compared with HIPK2^{low} group, P < 0.01.			

Wnt/β-catenin signaling pathway, mice were transfected *in vivo* to overexpress HIPK2 in lung tissue. We found that bleomycin induced an enhanced expression of β-catenin and mesenchymal cell markers (α-SMA, collagen I, and collagen III) in the lung, furthermore, nuclear β-catenin expression increased markedly. These changes were attenuated *via* overexpression of HIPK2. These results indicate that HIPK2 overexpression suppresses the Wnt/β-catenin signaling pathway and reduces pulmonary fibrosis in bleomycin-induced lung fibrosis.

HIPK2 can function as a negative [32] or positive regulator [33] of Wnt signaling. Cell-type specificity and other signaling inputs will likely affect HIPK2-regulated Wnt signaling [32]. In a few instances, HIPK2 knock-down increases stabilization and concomitant translocalization of β-catenin to the nucleus, and transactivation of β-catenin targeted genes [21]. More often, HIPK2 positively regulates the Wnt pathway by preventing degradation of β-catenin and increasing the transcriptional activity of the β-catenin/TCF complex [27]. To further understand the mechanism of HIPK2 expression variations in lung fibroblasts, we created MLFs that stably overexpress and silence HIPK2. Increased HIPK2 expression suppressed MLFs activation, including decreased migration and proliferation capacity, enhanced apoptosis rate, and lowered mesenchymal markers expression; MLFs with downregulated HIPK2 expression yielded the opposite detection results. the β-catenin expression changed inversely with the HIPK2 expression level, decreased at high HIPK2 expression, and increased at low HIPK2 expression. These results suggest that HIPK2 can negatively regulate MLFs activation, which may be mediated by the Wnt/β-catenin signaling pathway.

XAV939 can specifically inhibit Wnt/β-catenin signaling activation [24]. After binding to tankyrase, XAV939 can maintain the integrity of the destruction complex by stabilizing the Axin2 structure [34] *via* inhibiting the activity of the end anchorage polymerase

PARP, leading to the degradation of β-catenin [35]. To further confirm the relationship between MLFs activation, HIPK2, and Wnt/ β-catenin, we established NC, HIPK2^{low}, and HIPK2^{low} + XAV939 MLF groups. We discovered that HIPK2^{low} + XAV939 group inversed all the characteristics driven by low expression of HIPK2. Compared to the HIPK2^{low} group, HIPK2^{low} + XAV939 group appeared to suppress cell migration, proliferation capacity, and mesenchymal markers expression but enhanced apoptosis. Simultaneously, β-catenin mRNA and protein expression were inhibited in the HIPK2+XAV939 group. This implies that XAV939 intervention in the Wnt/β-catenin signaling pathway attenuated the MLFs activation induced by HIPK2 gene downregulation, confirming that HIPK2 regulates MLFs activation *via* the Wnt/β-catenin signaling pathway.

In summary, our investigation reveals that low expression of HIPK2 promotes pulmonary fibrosis and lung fibroblast activation *via* the Wnt/β-catenin signaling pathway, whereas HIPK2 overexpression suppresses pulmonary fibrosis development and Wnt/β-catenin signaling pathway inhibitor suppresses lung fibroblast activation. Although the experiment was limited to MLFs and bleomycin-induced pulmonary fibrosis mouse models, HIPK2 and Wnt/β-catenin signaling pathways as potential therapeutic targets for pulmonary fibrosis are worth additional investigation.

Funding

Author contributions

Fangfang Wang, Yanan Zhang, and Jing Ren finished all these experiments. Fangfang Wang and Wencheng Yu designed this research and wrote this paper. All

authors have read and agreed to the published version of the manuscript.

Conflict of interest

The authors declare that there are no competing interests associated with the manuscript.

References

1. Deng KM, Yang XS, Luo Q, et al. Deleterious role of Th9 cells in pulmonary fibrosis. Cells. 2021; 10(11), doi: 10.3390/cells10113209, indexed in Pubmed: 34831433.

2. Lee HY, Cho J, Kwak N, et al. Prognostic impact of malignant diseases in idiopathic pulmonary fibrosis. Sci Rep. 2020; 10(1): 18260, doi: 10.1038/s41598-020-75276-2, indexed in Pubmed: 33106517.

3. Sgalla G, Iovene B, Calvello M, et al. Idiopathic pulmonary fibrosis: pathogenesis and management. Respir Res. 2018; 19(1): 32, doi: 10.1186/s12931-018-0730-2, indexed in Pubmed: 29471816.

4. Raghu G, Richeldi L, Thomson CC, et al. authors of the guideline, Idiopathic Pulmonary Fibrosis (an Update) and Progressive Pulmonary Fibrosis in Adults: An Official ATS/ERS/JRS/ALAT Clinical Practice Guideline, American Thoracic Society, European Respiratory Society, Japanese Respiratory Society, and Latin American Thoracic Society. Diagnosis of idiopathic pulmonary fibrosis. An official ATS/ERS/JRS/ALAT clinical practice guideline. Am J Respir Crit Care Med. 2018; 198(5): e44–e68, doi: 10.1164/rccm.201807-1255ST, indexed in Pubmed: 30168753.

5. Richeldi L, du Bois RM, Raghu G, et al. INPULSIS Trial Investigators. Efficacy of a tyrosine kinase inhibitor in idiopathic pulmonary fibrosis. N Engl J Med. 2014; 370(22): 2071–2082, doi: 10.1056/NEJMoa1402584, indexed in Pubmed: 24836310.

6. King TE, Bradford WZ, Castro-Bernardini S, et al. ASCEND Study Group. A phase 3 trial of pirfenidone in patients with idiopathic pulmonary fibrosis. N Engl J Med. 2014; 370(22): 2083–2092, doi: 10.1056/NEJMoa1402582, indexed in Pubmed: 24836312.

7. Raghu G, Rochwerg B, Zhang Y, et al. American Thoracic Society, European Respiratory society, Japanese Respiratory Society, Latin American Thoracic Association. An official ATS/ERS/JRS/ALAT clinical practice guideline: treatment of idiopathic pulmonary fibrosis. An update of the 2011 clinical practice guideline. Am J Respir Crit Care Med. 2015; 192(2): e3–19, doi: 10.1164/rccm.201506-1063ST, indexed in Pubmed: 26177183.

8. Kim YH, Choi CY, Lee SJ, et al. Homeodomain-interacting protein kinases, a novel family of co-repressors for homeodomain transcription factors. J Biol Chem. 1998; 273(40): 25875–25879, doi: 10.1074/jbc.273.40.25875, indexed in Pubmed: 9748262.

9. Müller JP, Klempnauer KH. The CDC37-HSP90 chaperone complex co-translationally degrades the nascent kinase-dead mutant of HIPK2. FEBS Lett. 2021; 595(11): 1559–1568, doi: 10.1002/1873-3468.14080, indexed in Pubmed: 33786814.

10. Jin X, Qing S, Li Q, et al. Prostate cancer-associated SPOP mutations lead to genomic instability through disruption of the SPOP-HIPK2 axis. Nucleic Acids Res. 2021; 49(12): 6788–6803, doi: 10.1093/nar/gkab489, indexed in Pubmed: 34133717.

11. Ricci A, Cherubini E, Ulivieri A, et al. Homeodomain-interacting protein kinase2 in human idiopathic pulmonary fibrosis. J Cell Physiol. 2013; 228(1): 235–241, doi: 10.1002/jcp.24129, indexed in Pubmed: 22689412.

12. Agnew C, Liu L, Liu S, et al. The crystal structure of the protein kinase HIPK2 reveals a unique architecture of its CMGC-insert region. J Biol Chem. 2019; 294(37): 13545–13559, doi: 10.1074/jbc.RA119.009725, indexed in Pubmed: 31341017.

13. Zhu W, Li J, Zhang Y, et al. Inhibition of HMGB1 Suppresses Hepatocellular Carcinoma Progression HIPK2-Mediated Autophagic Degradation of ZEB1. Front Oncol. 2021; 11: 599124, doi: 10.3389/fonc.2021.599124, indexed in Pubmed: 33747917.

14. Kuwano Y, Nishida K, Akaike Y, et al. Homeodomain-interacting protein kinase-2: a critical regulator of the DNA damage response and the epigenome. Int J Mol Sci. 2016; 17(10), doi: 10.3390/ijms17101638, indexed in Pubmed: 27689990.

15. Liu R, Das B, Xiao W, et al. A novel inhibitor of homeodomain interacting protein kinase 2 mitigates kidney fibrosis through inhibition of the tgf-1/smad3 pathway. J Am Soc Nephrol. 2017; 28(7): 2133–2143, doi: 10.1681/ASN.2016080841, indexed in Pubmed: 28220029.

16. Jin Y, Ratnam K, Chuang PY, et al. A systems approach identifies HIPK2 as a key regulator of kidney fibrosis. Nat Med. 2012; 18(4): 580–588, doi: 10.1038/nm.2685, indexed in Pubmed: 22406746.

17. He P, Yu ZJ, Sun CY, et al. Knockdown of HIPK2 attenuates the pro-fibrogenic response of hepatic stellate cells induced by TGF-β1. Biomed Pharmacother. 2017; 85: 575–581, doi: 10.1016/j.biopha.2016.11.066, indexed in Pubmed: 27890429.

18. Zheng H, Sun Y, Shu X, et al. Overexpression of microRNA-100-5p attenuates the endothelial cell dysfunction by targeting HIPK2 under hypoxia and reoxygenation treatment. J Mol Histol. 2021; 52(5): 1115–1125, doi: 10.1007/s10735-021-10002-4, indexed in Pubmed: 34213736.

19. Zhang F, Qi L, Feng Q, et al. HIPK2 phosphorylates HDAC3 for NF-κB acetylation to ameliorate colitis-associated colorectal carcinoma and sepsis. Proc Natl Acad Sci U S A. 2021; 118(28), doi: 10.1073/pnas.2021798118, indexed in Pubmed: 34244427.

20. Fan Y, Wang N, Chuang P, et al. Role of HIPK2 in kidney fibrosis. Kidney Int Suppl (2011). 2014; 4(1): 97–101, doi: 10.1038/kisup.2014.18, indexed in Pubmed: 26312158.

21. Kim EA, Kim JiE, Sung KiSa, et al. Homeodomain-interacting protein kinase 2 (HIPK2) targets beta-catenin for phosphorylation and proteasomal degradation. Biochem Biophys Res Commun. 2010; 394(4): 966–971, doi: 10.1016/j.bbrc.2010.03.099, indexed in Pubmed: 20307497.

22. Cheng W, Wang F, Feng A, et al. CXXC5 attenuates pulmonary fibrosis in a bleomycin-induced mouse model and MLFs by suppression of the CD40/CD40L pathway. Biomed Res Int. 2020; 2020: 7840652, doi: 10.1155/2020/7840652, indexed in Pubmed: 32337277.

23. Yu W, Song X, Liu Y. TRB3 regulates pulmonary interstitial fibrosis through the MAPK signaling pathway. Int J Clin Exp Pathol. 2019; 12(9): 3247–3257, indexed in Pubmed: 31934168.

24. Huang SMA, Mishina YM, Liu S, et al. Tankyrase inhibition stabilizes axin and antagonizes Wnt signalling. Nature. 2009; 461(7264): 614–620, doi: 10.1038/nature08356, indexed in Pubmed: 19759537.

25. Spagnolo P, Sverzellati N, Rossi G, et al. Idiopathic pulmonary fibrosis: an update. Ann Med. 2015; 47(1): 15–27, doi: 10.3109/07853890.2014.982165, indexed in Pubmed: 25613170.

26. Chanda D, Otoupalova E, Smith SR, et al. Developmental pathways in the pathogenesis of lung fibrosis. Mol Aspects Med. 2019; 65: 56–69, doi: 10.1016/j.mam.2018.08.004, indexed in Pubmed: 30130563.

27. Blaquiere JA, Verheyen EM. Homeodomain-interacting protein kinases: diverse and complex roles in development and disease. Curr Top Dev Biol. 2017; 123: 73–103, doi: 10.1016/bs.ctdb.2016.10.002, indexed in Pubmed: 28236976.

28. Cao H, Wang C, Chen X, et al. Inhibition of Wnt/β-catenin signaling suppresses myofibroblast differentiation of lung resident mesenchymal stem cells and pulmonary fibrosis. Sci Rep. 2018;

8(1): 13644, doi: 10.1038/s41598-018-28968-9, indexed in Pubmed: 30206265.

29. Lam AP, Flozak AS, Russell S, et al. Nuclear β-catenin is increased in systemic sclerosis pulmonary fibrosis and promotes lung fibroblast migration and proliferation. Am J Respir Cell Mol Biol. 2011; 45(5): 915–922, doi: 10.1165/rcmb.2010-0113OC, indexed in Pubmed: 21454805.

30. Swann JB, Happe C, Boehm T. Elevated levels of Wnt signaling disrupt thymus morphogenesis and function. Sci Rep. 2017; 7(1): 785, doi: 10.1038/s41598-017-00842-0, indexed in Pubmed: 28400578.

31. Li C, Zheng Xu, Han Y, et al. XAV939 inhibits the proliferation and migration of lung adenocarcinoma A549 cells through the WNT pathway. Oncol Lett. 2018; 15(6): 8973–8982, doi: 10.3892/ol.2018.8491, indexed in Pubmed: 29805633.

32. Wei G, Ku S, Ma GK, et al. HIPK2 represses beta-catenin-mediated transcription, epidermal stem cell expansion, and skin tumori-

genesis. Proc Natl Acad Sci U S A. 2007; 104(32): 13040–13045, doi: 10.1073/pnas.0703213104, indexed in Pubmed: 17666529.

33. Hikasa H, Sokol S. Phosphorylation of TCF proteins by homeodomain-interacting protein kinase 2. J Biol Chem. 2011; 286(14): 12093–12100, doi: 10.1074/jbc.m110.185280, indexed in Pubmed: 21285352.

34. Kulak O, Chen H, Holohan B, et al. Disruption of wnt/β-catenin signaling and telomeric shortening are inextricable consequences of tankyrase inhibition in human cells. Mol Cell Biol. 2015; 35(14): 2425–2435, doi: 10.1128/MCB.00392-15, indexed in Pubmed: 25939383.

35. Wang C, Zhu H, Sun Z, et al. Inhibition of Wnt/β-catenin signaling promotes epithelial differentiation of mesenchymal stem cells and repairs bleomycin-induced lung injury. Am J Physiol Cell Physiol. 2014; 307(3): C234–C244, doi: 10.1152/ajpcell.00366.2013, indexed in Pubmed: 24898581.